CHINESE OPTICS LETTERS

Vol. 21, No. 2 | February 2023

Linearized microwave downconversion link based on fast and intelligent impairment equalization for noncooperative systems

Zhiyu Chen (陈智宇)[1], Xin Zhong (钟 欣)[1], Lin Jiang (蒋 林)[2], Jiaxin Xu (徐嘉鑫)[1], Jingxian Liu (刘静娴)[1], Yan Pan (盘 艳)[3], and Tao Zhou (周 涛)[1*]

[1] Key Laboratory of Science and Technology on Electronic Information Control, Chengdu 610029, China

[2] Center for Information Photonics & Communications, School of Information Science & Technology, Southwest Jiaotong University, Chengdu 610031, China

[3] Science and Technology on Communication Security Laboratory, Institute of Southwestern Communication, Chengdu 610041, China

*Corresponding author: zhj_zht@163.com

Received July 28, 2022 | Accepted September 8, 2022 | Posted Online November 15, 2022

We experimentally demonstrated the use of intelligent impairment equalization (IIE) for microwave downconversion link linearization in noncooperative systems. Such an equalizer is realized based on an artificial neural network (ANN). Once the training process is completed, the inverse link transfer function can be determined. With the inverse transformation for the detected signal after transmission, the third-order intermodulation distortion components are suppressed significantly without requiring any prior information from an input RF signal. Furthermore, fast training speed is achieved, since the configuration of ANN-based equalizer is simple. Experimental results show that the spurious-free dynamic range of the proposed link is improved to 106.5 dB · $Hz^{2/3}$, which is 11.3 dB higher than that of a link without IIE. Meanwhile, the training epochs reduce to only five, which has the potential to meet the practical engineering requirement.

Keywords: microwave photonics; linearized downconversion link; intelligent impairment equalization; artificial neural network.

DOI: 10.3788/COL202321.023902

1. Introduction

Directly transmitting frequency downconverted signals over a photonic link, which is defined as a downconversion link, has been considered as an enabling solution to meet the demand of antenna remoting applications such as radio over fiber (RoF), cellular wireless networks, radar systems, and electronic reconnaissance systems[1–4] due to the convenience of digitalization and postprocessing. Nevertheless, the nonlinearity of the modulator is one of the main problems that may lead to the intermodulation distortion (IMD), in particular the third-order IMD (IMD3), which would degrade the spurious free dynamic range (SFDR)[5]. So far, several effective schemes have been reported to improve the linearity of downconversion links, including (i) employing cascaded modulators combined with an optical filter[6–8], and (ii) using one dual-polarization quadrature phase shift keying (QPSK) Mach–Zehnder modulator (MZM) and two photodetectors (PDs)[9]. However, most microwave photonic-based systems, in particular the array radar systems and electronic reconnaissance systems, are built up based on simple intensity modulation and direct detection (IM-DD). Such systems are barely upgraded by using previous approaches, since the fiber link almost needs to be reconstructed, resulting in high cost and complex configuration. In order to overcome such a problem, the linearized IM-DD links combined with digital signal postprocessing have been proposed[10,11]. However, they could not be applied to a noncooperative system, where the frequency, bandwidth, and modulation format of the transmitted signal are unknown.

Artificial intelligence, on the other hand, has been a topic of extensive research in signal processing[12]. Based on artificial neural networks (ANNs) or deep learning, nonlinearity monitoring[13], integrated devices design[14], modulation formats identification[15,16], and link linearization[17] in photonic systems have been demonstrated with the advantages of high speed, simple hardware, and high flexibility. Consequently, an intelligent receiver that could linearize the microwave downconversion link would be one major characteristic in next-generation microwave photonic systems. However, the training speed and the information processing speed of ANNs become a practical problem for the application of microwave downconversion in noncooperative systems.

In this study, a simple linearized photonic downconversion link for microwave signals is proposed and experimentally demonstrated by using fast and intelligent impairment equalization (IIE). Such an equalizer only consists of a three-layer ANN. With supervised learning, the inverse link transfer function can be trained successfully. Transforming the detected signals by using such an inverse function, the downconversion link linearity can be enhanced. Different from the previous approach in Ref. [17], there is no need to do the complex Fourier transforms in the proposed method, since the inputs of the equalizer are an intermediate frequency (IF) signal in the time domain, instead of a radio-frequency (RF) signal in the frequency domain. Furthermore, fast training and information processing are achieved, since the configuration of the intelligent equalizer is simple. In addition, the proposed technique does not require any prior information from the input RF signal when the training process is completed, and thus, could be applied to noncooperative systems. Experimental results show that ~15 dB IMD3 suppression is achieved with the RF input power of 7 dBm per tone. Furthermore, the proposed link has an SFDR of 106.5 dB · $Hz^{2/3}$, which is 11.3 dB more than that of a link without impairment equalization. Meanwhile, the training epochs reduce to only five.

2. Principle

The principle of the proposed linearized downconversion link is shown in Fig. 1. Assuming the modulation coefficients of input RF signal and local oscillator (LO) signal are m_1 and m_2, respectively, the downconverted IF signal $i|_\Omega$ after dual-electrode MZM (DE-MZM) and direct detection can be expressed as[10]

$$i|_\Omega = 4\Re P_c J_1(m_1) J_1(m_2) \cos\phi \cos \Omega t, \tag{1}$$

where $\Re$, P_c, and Ω are the responsivity of the photodetector (PD), the input optical power, and the frequency of the downconverted signal, respectively. ϕ denotes the phase difference between two arms of DE-MZM induced by DC bias. As can be seen from Eq. (1), the bandwidth of the proposed link only depends on that of the PD.

By Taylor-expanding the Bessel function containing the term of m_1 in Eq. (1), the component of the downconverted signal becomes

$$i|_\Omega = \left(2m_1 - \frac{1}{4}m_1^3\right)\Re P_c J_1(m_2) \cos\phi \cos \Omega t. \tag{2}$$

According to Eq. (2), the transfer function of such a link is illustrated as Fig. 1, where the nonlinearity (i.e., harmonic) induces the IMD3 components.

In order to achieve the high linearity of the link, the inverse transfer function shown as in Fig. 1 (i.e., the red line) should be estimated accurately, which is the outstanding ability of an ANN-based equalizer. Different from the previous digital post-processing approaches, IMD3 compensation based on such an equalizer does not require any information of the transmission

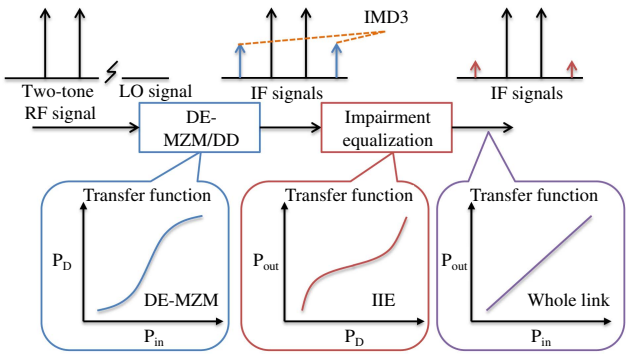

Fig. 1. Simplified diagram of linearized downconversion link and corresponding signal spectra and transfer characteristics. DE-MZM/DD, dual-electrode Mach–Zehnder modulated direct detection; IMD3, third-order intermodulation distortion; IIE, intelligent impairment equalization; RF, radio frequency; IF, intermediate frequency.

link. Moreover, this method does not require any prior information from the input RF signal either when the training process is completed.

The equalization-based inverse link transfer function estimation, which can be considered as a black box, is illustrated as Fig. 2. The architecture is a three-layer multilayer perceptron that consists of an input layer, a hidden layer, and an output layer. In the proposed scheme, only one neuron in the input and output layers is required, while the number of neurons in the hidden layer is 20. The activation functions $f(\cdot)$ and $g(\cdot)$ are a tangent sigmoid function for hidden layer neurons and a linear function for the output layer neurons, respectively. In this case, the outputs of the hidden layer (i.e., u_i) and the output layer (i.e., y) can be expressed as

$$u_i = f(V_i x + c_i), \tag{3}$$

$$y = g\left(\sum_{i=1}^{N} W_i u_i + b\right), \tag{4}$$

where V_i and W_i are weights of the hidden and output layers, c_i and b are bias values of the hidden and output layers, and x is the

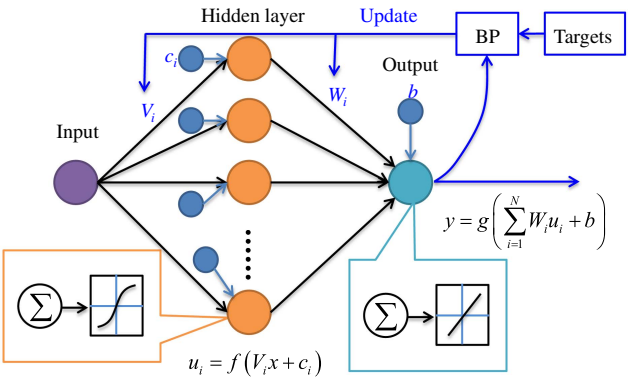

Fig. 2. Equalization-based inverse link transfer function estimation. BP, backpropagation.

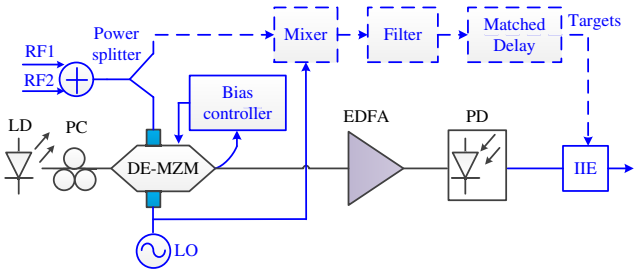

Fig. 3. Experimental setup of proposed linearized microwave downconversion link. LD, laser diode; PC, polarization controller; DE-MZM, dual-electrode Mach–Zehnder modulator; LO, local oscillator; EDFA, erbium-doped fiber amplifier; PD, photodetector; IIE, intelligent impairment equalization.

input vectors. Finally, a supervised learning method called back-propagation (BP) is utilized for training of such an intelligent equalizer (i.e., updating weights V_i and W_i) by comparing the output vectors y and targets vectors T, which are the initial downconverted signals without transmitting DE-MZM/DD link. The training process is completed when the mean square error (MSE) $\|y - T\|^2$ achieves the predetermined value. Once the weights are determined, the inverse link transfer function could be obtained according to Eq. (4).

3. Experimental Setup

The experimental setup is illustrated in Fig. 3. A light source at 1550 nm with the power of 8 dBm is modulated by a DE-MZM that is driven by a two-tone RF signal and an LO signal. On the one hand, those RF signals are downconverted directly by a wideband mixer. Subsequently, such signals as target vectors are sent to an IIE through a low-pass filter and a delay line. On the other hand, the RF signals and LO signal are converted to an optical signal, and then are amplified by an erbium-doped fiber amplifier (EDFA). Afterwards, such an optical signal is detected by a PD with a responsivity of 6 V/W (including an amplifier) and a 15 GHz bandwidth. In the experiment, the frequencies of the two-tone RF and LO signals are set to be 2.11, 2.13, and 2.5 GHz, respectively. In this case, the downconverted signals with the frequencies of 0.37 and 0.39 GHz are generated after the PD. Finally, such signals are digitalized by a real-time oscilloscope running at 40 GS/s, and then processed in an IIE with the target vectors, where the highly linear downconverted link can be achieved. In addition, the DE-MZM needs to be biased at the quadrature point by utilizing a bias feedback controller, which could stabilize the link transfer function.

4. Results and Discussion

In the experiment, the overall data comprising 800,002 photocurrent vectors from the oscilloscope are divided into two distinct subsets, including training and testing data sets. Among them, the length of the training subset is set to be 10,000, as well as that of the target vectors. Once the training phase is completed, the whole link transfer function is determined. In this case, a linearized microwave downconversion link is realized without requiring any prior information.

Figure 4(a) shows the MSE during the training phase as a function of the number of epochs, which are the steps in the ANN training process. Obviously, the MSE decreases with an increase in the number of epochs. As can be seen from the inset of Fig. 4(a), the IMD3 components are observed when the MSE is 10^{-6}, since the inverse transfer function fitted by the ANN deviates from the theoretical calculation. Therefore, as the predetermined MSE value decreases to 10^{-7}, the best training performance could achieve 3.2×10^{-8} at epoch 5. In this case, the measured training time for 10,000 points is approximately 2.3 s, while the testing time for 200,000 points is only 0.12 s, which indicates that the fast training speed and information processing speed are achieved. Compared to the approach in Ref. [17], the faster convergence speed is obtained by using the proposed IIE.

In order to estimate the effectiveness of IIE, the DE-MZM/DD transmission link and inverse link transfer characteristics are shown in Fig. 4(b), where the theoretical inverse transfer

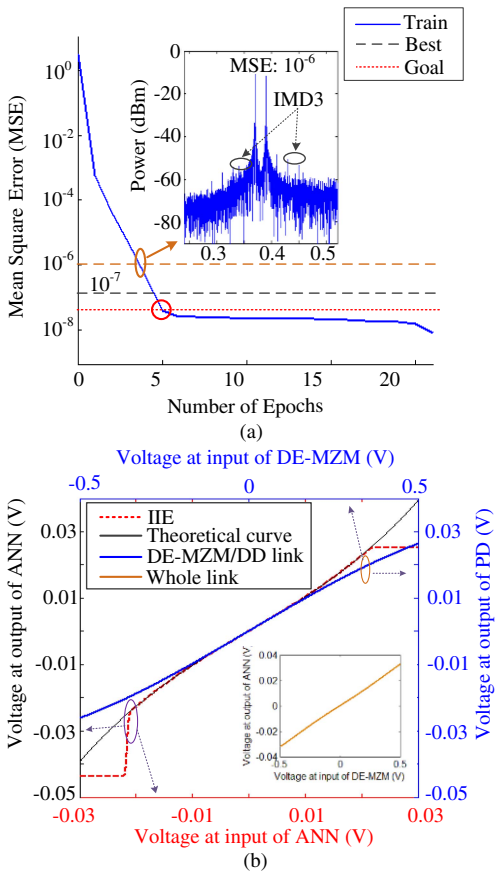

Fig. 4. (a) Dependence of MSE on the number of epochs for the training subsets; inset, the electrical spectrum of two-tone signal with the MSE of 10^{-6}; (b) DE-MZM/DD-based transmission link and calculated inverse link transfer functions; black solid curve, theoretical inverse transfer function; red dotted curve, IIE-based inverse link transfer function; inset, whole downconversion link transfer characteristic by applying IIE.

function calculated by Eq. (2) is also presented. It is evident that the IIE-based fitting curve (i.e., the red dotted line) that agrees well with the theoretical calculation (i.e., the black solid line), presents the inverse characteristic of the DE-MZM/DD link. By applying this inverse function, the whole link transfer characteristic after compensation is illustrated in the inset of Fig. 4(b), which indicates that the highly linear microwave downconversion link is realized.

Figures 5(a) and 5(b) show the electrical spectra before and after applying IIE when the input two-tone frequencies are 2.11 and 2.13 GHz. For the first case, strong IMD3 components are observed when the RF input power is 7 dBm per tone. These two components are hardly mitigated by using electrical filters due to the small frequency space between them and the fundamental products. However, the IMD3 suppression of 15 dB is achieved, while the powers of fundamental products keep constant by applying the IIE. In addition, the electrical spectra are measured as shown in Figs. 5(c)–5(f) when the frequencies of the input two-tone RF signals are changed to be 2.1, 2.14 GHz and 4.11, 4.13 GHz, respectively. In these cases, the ANN is still trained by using two-tone signals with the frequency of 2.11 and 2.13 GHz. As can be seen, the IMD3 components are also suppressed significantly after compensation with the proposed IIE, which indicates that such an ANN can also work for the two-tone RF signals with other frequencies.

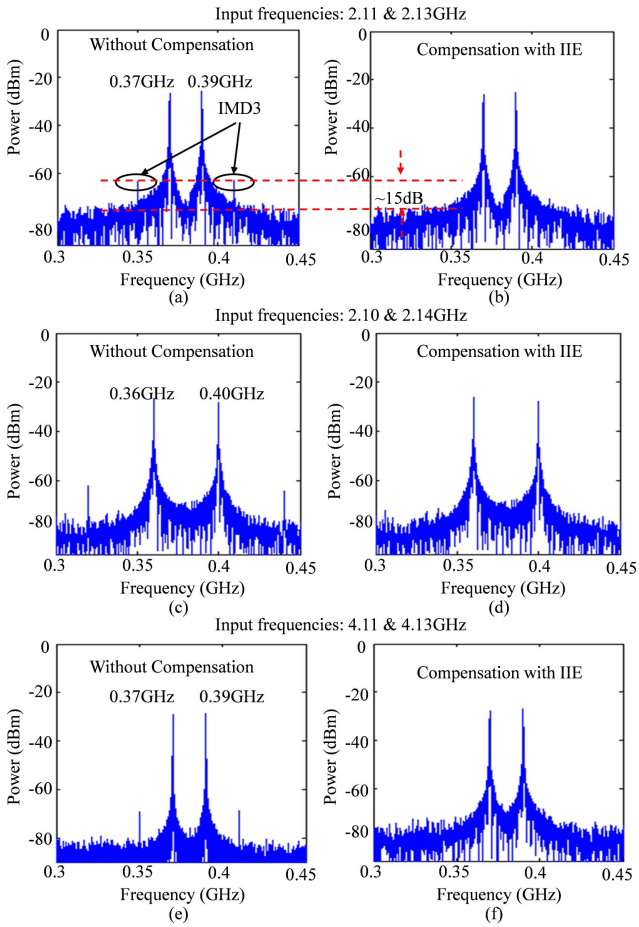

Fig. 5. Electrical spectra of the two-tone input tests before and after applying IIE when the frequencies are set to be (a), (b) 2.11 GHz and 2.13 GHz; (c), (d) 2.10 GHz and 2.14 GHz; and (e), (f) 4.11 GHz and 4.13 GHz, respectively.

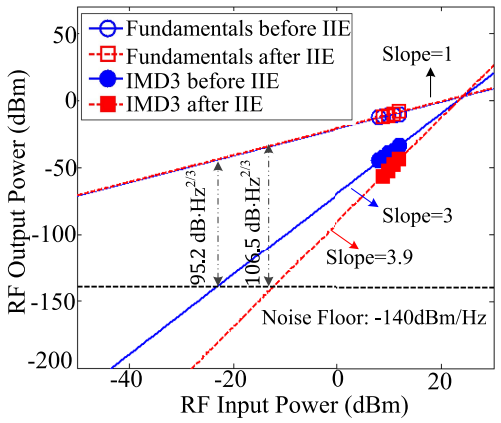

Fig. 6. Measured SFDR before (solid line) and after (dashed line) IIE.

In order to further verify the performance of the SFDR, the link transfer functions are trained by using the proposed IIE when the input RF power changes from 8 dBm to 12 dBm. In this case, the SFDRs before and after IIE are shown in Fig. 6. As can be seen, the SFDR before linearization is 95.2 dB · $Hz^{2/3}$, with a measured noise floor of −140 dBm/Hz. After equalization, the SFDR increases to 106.5 dB · $Hz^{2/3}$.

5. Conclusion

In conclusion, a linearized downconverted microwave photonic link based on fast and IIE is theoretically analyzed and experimentally demonstrated. With the supervised learning, the whole transfer function of the link can be linearized. Experimental results show that an IMD3 suppression of 15 dB is achieved, and the training epochs reduce to only five. Furthermore, the SFDR is improved from 95.2 dB · $Hz^{2/3}$ to 106.5 dB · $Hz^{2/3}$. The proposed linearization method is highly promising in non-cooperative RoF systems.

Acknowledgement

This work was supported in part by the National Key Research and Development Program of China (No. 2018YFB2201702), the National Natural Science Foundation of China (Nos. U21A20507 and 62005228), and the Fundamental Research Funds for the Central Universities (No. 2682021CX050).

References

1. P. Ghelfi, F. Laghezza, F. Scotti, G. Serafino, A. Capria, S. Pinna, D. Onori, C. Porzi, M. Scaffardi, A. Malacarne, V. Vercesi, E. Lazzeri, F. Berizzi, and A. Bogoni, "A fully photonics-based coherent radar system," Nature **507**, 341 (2014).

2. Z. Y. Chen, T. Zhou, X. Zhong, J. X. Liu, M. W. Wang, and J. Ye, "Stable downlinks for wideband radio frequencies in distributed noncooperative system," J. Light. Technol. **36**, 4514 (2018).
3. J. J. Zhao, T. Liu, B. Wang, and W. K. Zhang, "Distributed phase synchronization transmission based on fiber," Electr. Inf. Warfare Technol. **34**, 64 (2019).
4. H. Mao, "Information processing method of electronic warfare events based on communication technology," Secur. Commun. Netw. **2022**, 9309710 (2022).
5. Z. Y. Chen, L. S. Yan, W. Pan, B. Luo, X. Zou, Y. H. Guo, H. Y. Jiang, and T. Zhou, "SFDR enhancement in analog photonic links by simultaneous compensation for dispersion and nonlinearity," Opt. Express **21**, 20999 (2013).
6. Y. Y. Li, A. J. Wen, and D. J. Shan, "An analog photonic down-conversion link with simultaneous IMD3 distortion suppression and dispersion-induced power fading compensation," J. Light. Technol. **38**, 3908 (2020).
7. G. F. Li, T. Shang, T. Gao, Y. L. Zhang, and D. Chen, "Photonic downconversion link with linearization and full spectrum utilization," in *Proceedings of Topical Meeting on Microwave Photonics (MWP)* (2017), paper THP.2.
8. X. Zhu, T. Jin, H. Chi, G. C. Tong, D. Li, L. L. Zou, W. M. Liu, and Y. Fu, "Photonic down-conversion and linearization with tunable IF bandwidth and improved spurious-free dynamic range," Electron. Lett. **55**, 105 (2019).
9. Z. Niu, H. Yu, M. Chen, P. Li, H. Chen, and S. Xie, "High linearity down-converting analog photonic link based on digital signal post-compensation," in *Optical Fiber Communication Conference* (2014), paper W2A.37.
10. Y. Pan, L. S. Yan, Z. Y. Chen, W. Pan, B. Luo, X. H. Zou, J. Ye, and A. L. Yi, "Adaptive linearized microwave downconversion utilizing a single dual-electrode Mach-Zehnder modulator," Opt. Lett. **40**, 2649 (2015).
11. P. X. Li, W. Pan, X. H. Zou, W. L. Bai, Y. Pan, X. Y. Han, and L. S. Yan, "Fast self-adaptive generic digital linearization for analog microwave photonic systems," J. Light. Technol. **39**, 7894 (2014).
12. Y. LeCun, Y. Bengio, and G. Hinton, "Deep learning," Nature **521**, 436 (2015).
13. M. Lonardi, J. Pesic, P. Jenneve, P. Ramantanis, N. Rossi, A. Ghazisaeidi, and S. Bigo, "Optical nonlinearity monitoring and launch power optimization by artificial neural networks," J. Light. Technol. **38**, 2637 (2020).
14. A. M. Hammond and R. M. Camacho, "Designing integrated photonic devices using artificial neural networks," Opt. Express **27**, 29620 (2019).
15. F. N. Khan, K. Zhong, X. Zhou, W. H. Al-Arashi, C. Y. Yu, C. Liu, and A. P. T. Lau, "Joint OSNR monitoring and modulation format identification in digital coherent receivers using deep neural networks," Opt. Express **25**, 17767 (2017).
16. M. Hao, L. S. Yan, A. L. Yi, L. Jiang, Y. Pan, W. Pan, and B. Luo, "Stokes space modulation format identification for optical signals using probabilistic neural network," IEEE Photon. J. **10**, 7202213 (2018).
17. E. J. Liu, Z. M. Yu, Z. Q. Wan, L. Shu, K. X. Sun, L. L. Gui, and K. Xu, "Linearized wideband and multi-carrier link based on TL-ANN," Chin. Opt. Lett. **19**, 113901 (2021).